PM10 source apportionment in the surroundings of the San Vicente del Raspeig cement plant complex in southeastern Spain

Environ Sci Pollut Res (2011) 18:64–74
DOI 10.1007/s11356-010-0352-9

RESEARCH ARTICLE

PM_{10} source apportionment in the surroundings of the San Vicente del Raspeig cement plant complex in southeastern Spain

Eduardo Yubero · Adoración Carratalá · Javier Crespo · Jose Nicolás · Milagros Santacatalina · Silvia Nava · Franco Lucarelli · Massimo Chiari

Received: 2 February 2010 / Accepted: 31 May 2010 / Published online: 19 June 2010

Abstract
Introduction The concentrations of trace metals, ionic species, and carbonaceous components in PM_{10} (particulate matter with aerodynamic diameters smaller than 10 μm) were measured from samples collected near an industrial complex, primarily composed of cement plants, in southeastern Spain, from September 2005 to August 2006.
Materials and methods Positive matrix factorization and conditional probability function were applied to this data set to identify different types of sources.
Results Six significant sources were identified: crustal matter, traffic, aged sea salt, industrial emissions, secondary aerosol, and sea salt. The difficulty of separating anthropogenic sources from those of natural origin is highlighted in this study; in particular, the crustal source can be connected with both natural (African outbreaks, wind resuspension) and man-made emissions, like fugitive emissions in an industrial environment.

Responsible editor: Euripides Stephanou.

E. Yubero (✉) · J. Crespo · J. Nicolás
Laboratory of Atmospheric Pollution (LCA),
Miguel Hernández University,
Av. de la Universidad s/n, Edif. Alcudia,
03202 Elche, Spain
e-mail: eyubero@umh.es

A. Carratalá · M. Santacatalina
Department of Chemical Engineering, University of Alicante,
P. O. Box 99, 03080 Alicante, Spain

S. Nava · F. Lucarelli · M. Chiari
Physics Department, University of Florence and INFN,
via Sansone 1,
1-50019 Sesto Fiorentino, Italy

Keywords PM_{10} · PMF · CPF · Cement plant

1 Introduction

In recent years, frenetic construction activity, above all in countries like Spain, has forced industrial providers of construction supplies like cement plants, ceramic and metallurgical industries, etc. to greatly increase their production to meet the great demand for materials. The manufacture of these materials has released great quantities of atmospheric contaminants into the environment, including heavy metals, volatile organic compounds, gases, etc. Due to the potential impact that these contaminants may have upon the human body and ecosystem, particles with diameters inferior to 10 μm (PM_{10}) are particularly important as carriers of harmful trace elements like As, Cd, Cu, Cr, Mn, Ni, Pb, and Zn (Natusch et al. 1974; Dockery and Pope 1994); furthermore, these are highly associated with anthropogenic activity. Many studies exist relating increases in mortality with increases in PM_{10} levels. For example, a significant association between PM_{10} and lung cancer has been demonstrated (Abbey et al. 1999): In particular, it has been established that an increase of 10 $\mu g/m^3$ in PM_{10} concentrations may cause a 1% increase in general mortality (Lippmann 1998). In general, particulate matter can be produced from sources both natural (long-range transport from arid zones, marine aerosol, dust resuspension from wind, etc.) and anthropogenic (traffic, industry, incinerators, etc.). In an effort to reduce social costs and develop efficient administration regulatory policies for these contaminants, a precise and rapid evaluation of the emission sources of particulate matter is greatly desired.

Receptor models are evaluation methods of particulate matter sources based on the analysis of the chemical species present at a receptor site. Among different multivariate receptor models, principal component analysis (PCA) and factor analysis (FA) have been used frequently since the 1970s. These methods are capable of identifying aerosol sources with the help of different commercial statistical programs in a relatively simple and precise manner (Salvador et al. 2007). However, as PCA and FA depend solely upon the covariance matrix, a general requirement for the contribution of each source is not met, e.g., negative values for factor loading and the factor scores may be obtained. Positive matrix factorization (PMF) is a new model based on a weighted non-negative least squares algorithm which overcomes this problem as it beforehand restricts the mentioned values in such a way that only positive values are allowed; moreover, experimental concentrations are weighted using their uncertainties. PMF has already been applied in numerous studies (Polissar et al. 1998; Kim et al. 2004; Kim and Hopke 2004b; Begum et al. 2004; Nicolás et al. 2008). The disadvantages of PCA (or FA) and advantages of advanced receptor models like PMF have been compared in different studies (e.g., Qin et al. 2002; Viana et al. 2008; Tauler et al. 2009).

The objective of this work was to identify the natural and anthropogenic sources affecting the studied zone (marine aerosol, Saharan outbreaks, traffic, industrial emissions, dust), and consequently the surrounding residential areas, and quantify their contribution by means of PMF.

2 Materials and methods

2.1 Site characteristics and sampling

The cement plants are adjacent to the cities of San Vicente del Raspeig (38°25′25″ N, 0°31′20″ W, 65,000 inhabitants) and Alicante (38°20′43″ N, 0°28′59″ W, 350,000 inhabitants) in southeastern Spain. Because of this proximity, dangerous atmospheric pollutants emitted from these industrial sources can seriously affect the surrounding areas. The sampling took place on the roof of a four-story building on the University of Alicante campus (see Fig. 1) located near the two cement plants. The two plants' manufacturing processes differ; the nearest one, in operation since the 1920s, has been producing in recent years only white cement based on the semi-humid process, while the other produces gray cement and has been operational since 1960 using dry technology and a precalcinator. Both plants operate throughout the entire year, 24 h a day, slowing or stopping production only for maintenance concerns.

At the study location, the meteorological conditions have predominantly northwesterly winds, except during the summer season when a sea breeze is common. The sampler location, downwind of the two plants, allowed evaluating their influence upon local pollution (Fig. 1). Numerous quarries in nearby areas supply the industrial complex with the necessary raw materials using the customary semi-trailer trucks.

On the other hand, due to its proximity to the African continent, the study area receives significant contributions of particulate matter from Africa. In fact, approximately 16% of the air masses reaching the sampling site have North African origins (Querol et al. 2008). Moreover, due to the proximity of the Mediterranean Sea, the marine aerosol surely has an impact on PM_{10}.

One hundred twenty samples were collected on quartz fiber filters by a high-volume Digitel DL77 sampler. The sampling took place between September 2005 and August 2006. The number of samples collected each month was the same, measuring on one of every 3 days, weekends included. The samples are representative of the occurrence of Saharan outbreaks, precipitation, and any special events occurring during one entire year (like high pollution episodes). In this way, approximately one third of the outbreaks and high-pollution days that took place in this period were analyzed. PM_{10} mass was gravimetrically determined by a 10-μg sensitive microbalance located in a temperature- and humidity-controlled chamber (20°C, 50% RH) where the filters were conditioned for 24 h before weighing, both before and after the sampling.

2.2 Analysis of metal, ionic, and carbonaceous components

The concentrations of trace metals, ionic species, and carbonaceous compounds from the PM_{10} samples were analyzed by inductively coupled plasma atomic emission spectroscopy (ICP-AES), ICP mass spectrometry (ICP-MS), ion chromatography (IC), and thermal optical transmittance analysis (TOT).

Major (Fe, Al, Mg, Ca) and trace (V, Ni, Mn, Pb, Ba, Ti, Tl, Sb, Sr, Cu) metal concentrations were determined from the solution obtained after digesting a portion of the filter with a digestion oxidant (HNO_3 (65%) + H_2O_2 (30%)) in a microwave oven reaching a high temperature (170°C) by ICP-AES and ICP-MS. A few milligrams of reference material NIST 1648 were added to a fraction of a blank filter to confirm the accuracy of the acidic digestions analysis. The recovery percentage of the reference material is within the range of 85–105% for all elements analyzed.

Anion (SO_4^{2-}, NO_3^-, Cl^-) and cation (Na^+, NH_4^+, K^+, Mg^{2+}, Ca^{2+}) concentrations were analyzed by IC (DIONEX DX-20). The anion separation column was an AS9-HC 250 × 4 mm, with Na_2CO_3 9 mM as eluent, running at

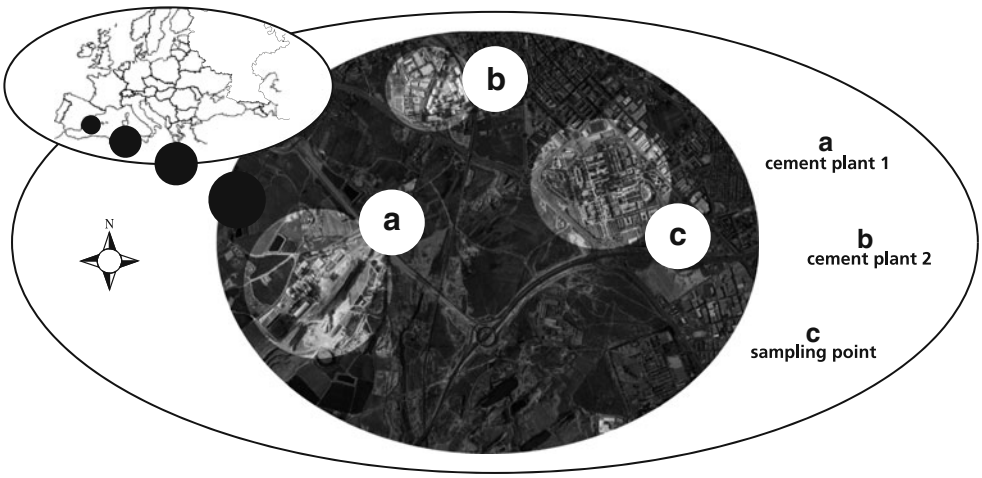

Fig. 1 Location of the sampling point and cement plants

1.4 mL min^{-1}. Cation analysis was performed using a CS12A 250 × 4-mm cationic column and 20 mM methanesulfonic eluent at a flow rate of 0.8 mL min^{-1}.

One punch (area 1.5 cm^2) cut from each quartz filter was analyzed by the TOT method (Sunset Inc.; Birch and Cary 1996) to quantify elemental and organic carbon (EC and OC). The analysis was carried out following the NIOSH 5040 protocol. The technique detection limit was 0.2 μg C cm^{-2} and the precision was ~5%.

Fractions of the blank filters were analyzed in the batches of their respective filter samples and the corresponding blank concentrations were subtracted from each sample.

The concentrations of carbon carbonate (CC), insoluble Ca, and Mg were also calculated in an indirect manner. First, the CC was obtained by the calculation of the ionic balance: It was assumed that the amount of non-analyzed anions was due to the presence of either carbonate or bicarbonate. Since in TOT measurements the CC contribution is included in the OC concentration, this soluble CC concentration was subtracted from the OC quantity obtained by TOT. For the calculation of insoluble Ca and Mg, the Ca and Mg obtained by IC (soluble) was directly subtracted from that obtained by ICP (total).

Table 1 shows the measured average concentrations along with their maximum and minimum values as well as the number of samples below this limit. Elements presenting a signal-to-noise ratio (S/N) <2 have not been shown and have not been used for statistical analysis.

2.3 Positive matrix factorization and conditional probability function

The PMF technique, developed by Paatero and Tapper (Paatero and Tapper 1994; Paatero 2004), is an advanced receptor model which solves the factor analysis problem by a least squares fit. Data values are weighted by realistic error estimates (optimum data point scaling), and non-negativity constraints are imposed in the factor computational process.

A conventional factor analysis model can be written as

$$X = GF + E \tag{1}$$

where X is the known $n \times m$ matrix of the m measured elements or chemical species in n samples. G is an $n \times p$ matrix of source contributions to the samples (time variations). F is a $p \times m$ matrix of source compositions (source profiles). E is defined as a residual matrix, i.e., the difference between the measurement X and the model Y as a function of factors G and F.

$$e_{ij} = x_{ij} - y_{ij} = x_{ij} - \sum_{k=1}^{p} g_{ik} f_{kj} \tag{2}$$

where i=1,…, n samples; j=1,…, m elements or chemical species; k=1,…, p sources.

The PMF objective is to minimize the sum of the squares of the residuals, inversely weighted with uncertainty estimates of the data points. The objective function to be minimized, $Q(E)$, is defined as

$$Q(E) = \sum_{i=1}^{m} \sum_{j=1}^{n} \left[\frac{e_{ij}}{s_{ij}} \right]^2 \tag{3}$$

where s_{ij} is an uncertainty estimate in the jth element measured in the ith sample. Furthermore, PMF constrains all the elements of G and F to be non-negative, meaning that the chemical species cannot give negative contributions to the source profiles ($f_{kj} \geq 0$) and that the sources cannot give negative mass contributions ($g_{ik} \geq 0$). The solution of Eq. 3 is obtained by the PMF2 algorithm in which both matrices G and F are adjusted in each iteration step. This process continues until convergence occurs (Paatero 1997).

The Polissar et al. (1998) procedure was used to assign measured data and associated uncertainties as the

Table 1 Summary of chemical compositions (in ng m^{-3})

Elements	Mean	Min	Max	SD	BDL (%)
SO_4^{2-}	4,235	1,246	16,064	2,349	0
NO_3^-	2,704	386	8,769	1,751	0
NH_4^+	589	43	4,751	719	0
EC	1,148	218	3,852	613	0
OC	2,377	97	7,926	1,551	3
CC	591	40	2,265	415	6.6
Cl^-	913	87	3,807	698	0
Na^+	778	96	2,914	628	0
K^+	331	65	968	180	0
Ca_{insol}	2,576	3.9	25,539	3,610	5
Ca_{sol}	3,134	86	7,711	1,576	8
Mg_{insol}	144	0.41	861	157	14
Mg_{sol}	132	32	369	79	9.7
Fe	383	77	1,214	214	0
Al	325	18	1,476	255	0
V	29	0.3	110	21	0
Ni	7.2	0.2	25	4.6	12.5
Cu	13	4.2	43	6.2	1.7
Pb	13	3.3	44	7.8	0
Mn	7.2	1.7	25	5.0	0.8
Ba	14	5.2	36	6.5	0
Sr	16	4.3	65	10	0
Ti	5.8	0.12	24	3.6	2.5
Tl	0.98	0.05	4.0	0.77	4.2
Sb	0.48	0.002	1.7	0.31	21

SD standard deviation, *BDL* below detection limit

PMF input data. The concentration values were used for the measured data and the sum of the analytical uncertainty, plus one third of the detection limit value, as the overall uncertainty assigned to each measured value. Values below the detection limit were replaced by half of the detection limit values, and their overall uncertainties were set as the sum of one half the average detection limits for this element and one third of the detection limit values.

Rotational ambiguity is always a problem in factor analysis (Paatero et al. 2002) because of the free rotation of matrices. In this work, PMF solutions were systematically explored (changing the F_{PEAK} value between −1 and 1 in increments of 0.1) and the resulting Q values, the scaled residuals, and the F and G matrices were examined to find the most reasonable solution. It should also be remembered that in PMF, the choice of factors is always a compromise because PMF is a descriptive model and there is no objective criterion to choose the ideal solution. Finally, the solution with six sources and PEAK = 0 was the most reasonable, as discussed in the following section. The scaled residuals (Paatero and Hopke 2003) were almost

Table 2 Brief summary of annual and seasonal PM_{10} concentrations (PM_{10} in µg m^{-3})

	Fall	Winter	Spring	Summer	All study periods
Mean	40.4	40.6	41.5	39.7	40.5
Median	34.6	38.3	35.7	37.5	37.0
SD	21.1	16.0	19.7	13.0	17.5
Min	15.9	17.3	20.4	21.7	15.9
Max	120	85.5	110	82.6	120
N	30	30	31	30	121
Days with SDE	0	0	11	8	19

SDE Saharan dust event

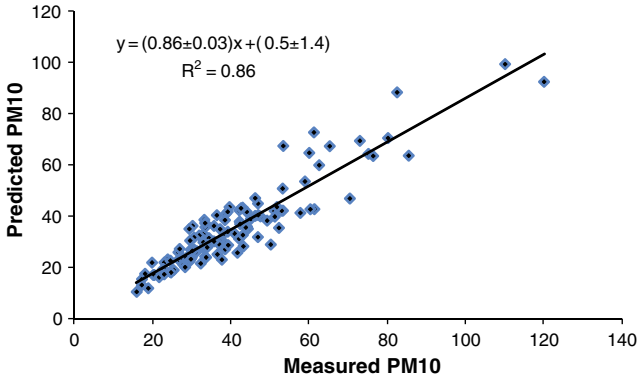

Fig. 2 Predicted (by PMF) versus measured PM_{10} mass concentration in micrograms per cubic meter

normally distributed and between ±3 for the majority of the species.

Multiple linear regression was applied to regress the total PM_{10} mass against the estimated source contributions (Hopke et al. 1980). The regression coefficients should all be positive if the resolved sources are reasonable. The estimated uncertainties of PM_{10} mass concentrations were set at four times their experimental value so that the large uncertainties decreased their weight in the model fit. The same was done for the concentrations of the variables that have been obtained indirectly (CC, insoluble Ca, and Mg).

Furthermore, conditioned probability functions (CPFs) were calculated in this study using wind direction and velocity, and the source characteristics were examined by evaluating the seasonal distribution of the contribution of each source. Developed by Ashbaugh et al. (1985), a CPF plot can be specifically used to determine possible local source regions using wind direction data (Begum et al. 2004; Kim and Hopke 2004a; Kim et al. 2004; Nicolás et al. 2009a). This method combines the contributions of each source from the PMF and meteorological data (wind direction and velocity) to evaluate the influence of a local source upon the receptor site. The CPF is calculated in the

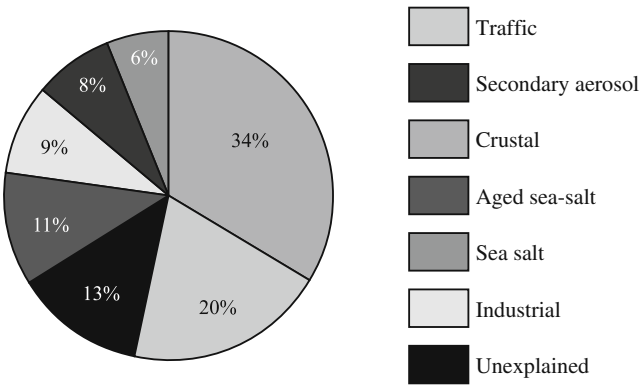

Fig. 3 Average source contribution to PM_{10}, obtained by PMF

Table 3 Summary of source contribution estimate for PM_{10}

Sources	$\mu g m^{-3}$			
	Mean	SD	Min	Max
Crustal	13.6	14.4	0.006	83.7
Traffic	7.9	6.3	0.003	35.8
Aged sea salt	4.4	4.1	0.001	29.8
Industrial	3.5	3.1	0.002	17.3
Secondary aerosol	3.4	4.4	0.001	29.8
Sea salt	2.3	2.3	0.001	16.7
Predicted	35.2	16.2	10.6	99.4
Measured	40.5	17.5	15.9	120

following manner:

$$\mathrm{CPF}_{\Delta\theta} = m_{\Delta\theta}/n_{\Delta\theta} \quad (5)$$

where $m_{\Delta\theta}$ indicates the frequency of winds blowing from direction $\theta \pm \Delta\theta/2$ on days with source concentrations above a threshold criterion, while $n_{\Delta\theta}$ indicates the wind frequency from direction $\theta \pm D\theta/2$. Therefore, the CPF is a probability value from 0 to 1, which can be subsequently used to estimate the source's possible location. In this study, the $\Delta\theta$ value was set at 30° and the threshold chosen was the average concentration. Calm periods (wind velocities below 1.2 m s^{-1}) were not included in this analysis.

3 Results and discussion

The average PM_{10} annual value (± the standard deviation) was 40.5 (±17.5) $\mu g\ m^{-3}$, and daily concentrations ranged between 15.9 and 120 $\mu g\ m^{-3}$ (see Table 2). This average annual concentration exceeds the annual limit value for PM_{10} established by the European Union of 40 $\mu g\ m^{-3}$ (Directive 2008/50/CE). At the same time, the daily limit value of 50 $\mu g\ m^{-3}$ was exceeded on 26 occasions of the 120 sampled days, and these days appear throughout the entire year. No PM_{10} seasonal tendency appears as the average value was similar in all four seasons. However, different processes determined the PM_{10} concentrations in the different seasons. During spring and summer, many long-range particulate transport events from Africa (Saharan dust) occur. In fall and winter, frequent thermal inversions and situations with ground fog help maintain poor air quality due to anthropogenic emissions.

Based on PMF source apportionment, the sources were classified into six categories. With the five-, six-, seven-factor solutions, and $F_{\mathrm{PEAK}} = 0$, the theoretical value Q

Fig. 4 PMF results: source profiles (*bars*) and explained variations (*squares*) ▶

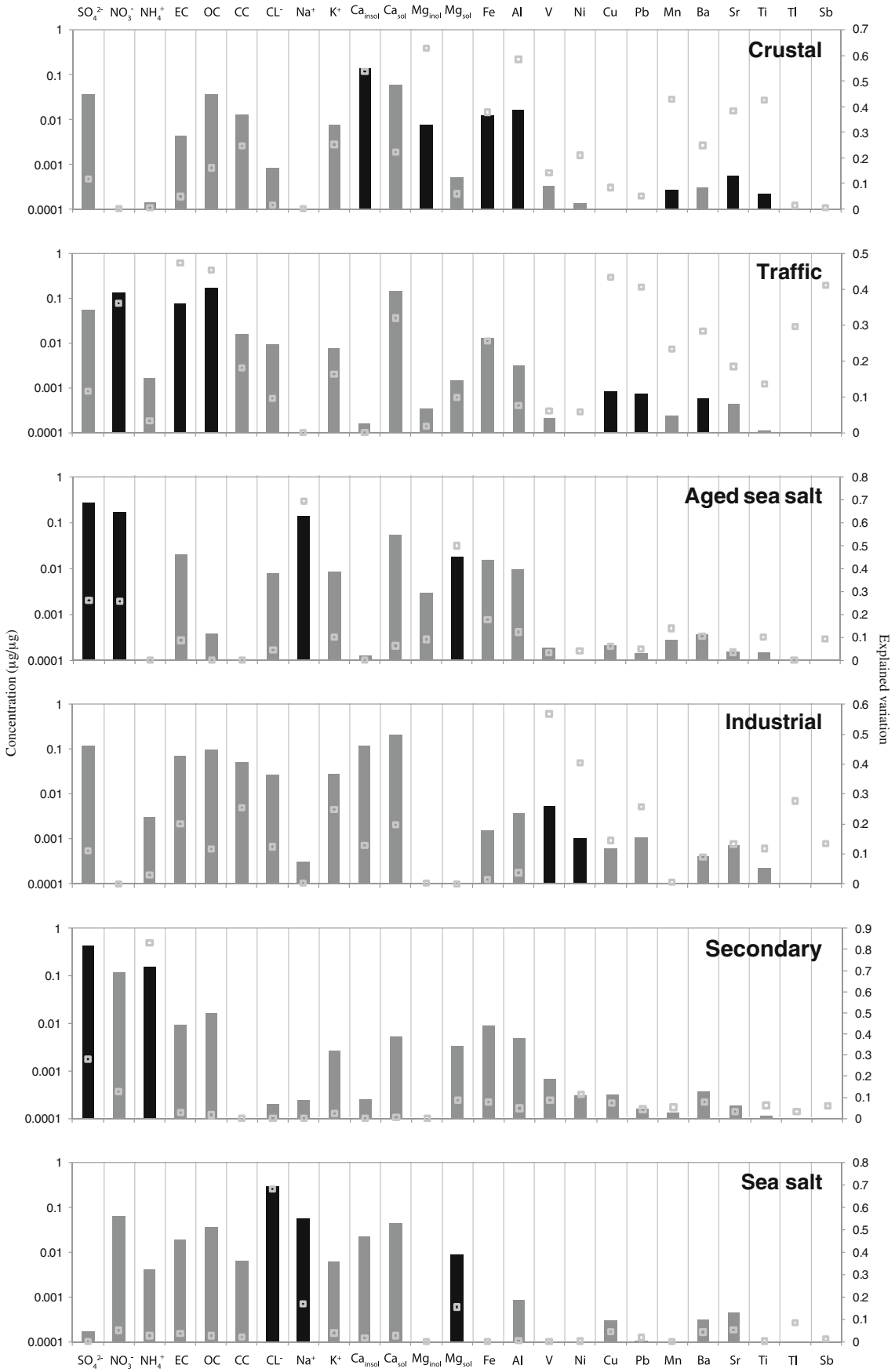
SO_4^{2-} NO_3^- NH_4^+ EC OC CC CL^- Na^+ K^+ Ca_{insol} Ca_{sol} Mg_{inol} Mg_{sol} Fe Al V Ni Cu Pb Mn Ba Sr Ti Tl Sb
Crustal
Traffic
Aged sea salt
Industrial
Secondary
Sea salt
Concentration (µg/µg)
Explained variation

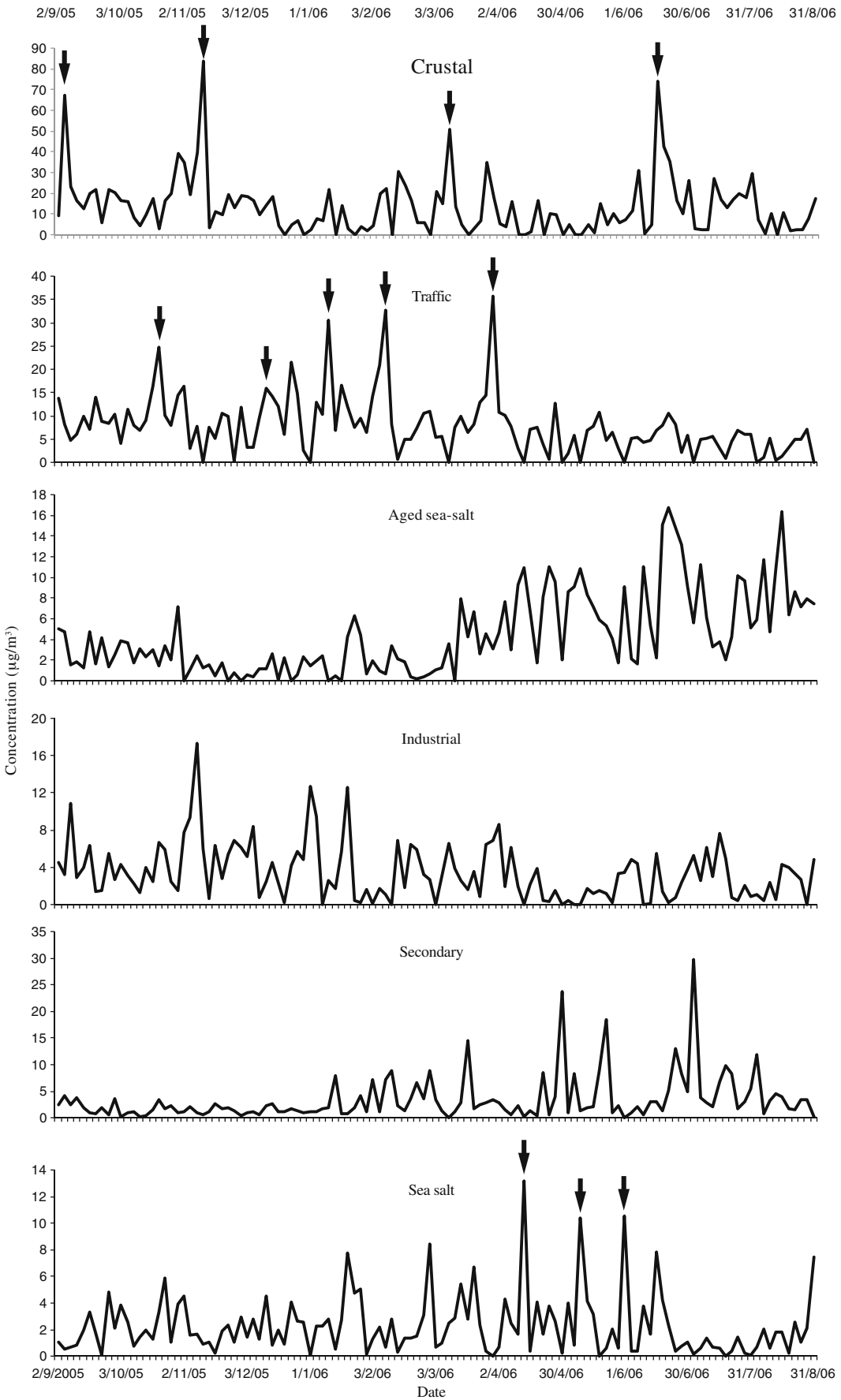
2/9/05
3/10/05
2/11/05
3/12/05
1/1/06
3/2/06
3/3/06
2/4/06
30/4/06
1/6/06
30/6/06
31/7/06
31/8/06
Crustal
Traffic
Aged sea-salt
Industrial
Secondary
Sea salt
Concentration (µg/m³)
Date

◀ **Fig. 5** PMF results: time trends of the source concentrations (the *arrows* indicate episodes that are discussed in the text)

(approximately equal to the degrees of freedom or number of input data points minus the number of the solution values) was approximately achieved. The only difference between the solution with five and six sources was that with five, crustal and industrial sources appeared in the same factor, while in the six-source solution, these two sources were separated. With the seven-factor solution, we obtained exactly the same sources found with six factors, plus a unique element source without any characteristic time pattern. As the origin of this source was not clear, we selected the six-factor solution.

Each source and its relative contribution, quantitatively calculated, are discussed next in the following. With six sources, 87% of the measured PM_{10} concentration is explained. The undetermined PM mass fraction could be attributed to non-C atoms of organic matter (Huerbert and Charlson 2000) and structural and absorbed water remaining during sample conditioning (EPA Air Quality Criteria for Particulate Matter). The determination coefficient (r^2) between the predicted and the measured PM_{10} concentration was 0.86 (Fig. 2).

The pie chart in Fig. 3 (and Table 3) presents the average contribution from each source during the sampling period. In Fig. 4, source profiles and explained variations (e.g., the percentages of each species represented by each source) are shown. The temporal contribution and seasonal average of the six sources to the PM_{10} mass concentration is reported in Figs. 5 and 6, respectively. Finally, the CPF results are presented in Fig. 7.

The first source provides the greatest contribution between all the sources with an average of 13.7 μg m^{-3} (34%) throughout the entire period. It is characterized primarily by Ca, both soluble as well as insoluble, insoluble Mg, Al, Mn, Sr and Ti, and, to a lesser extent, by Fe, K, and CC. Because of its composition, this source can be called "crustal," and there are three possible origins for it. The first one is that of Saharan intrusions; as aforementioned, they occur mostly in spring and summer (Nicolás et al. 2008). Dust resuspension from traffic, as well as wind, is another aspect that must be kept in mind. The area's ground surface is mostly made up of limestone, rich in calcium and magnesium carbonates. Moreover, scarce precipitation limits the cleansing of paved surfaces, and as a result, resuspension is favored (Amato et al. 2009). The third origin, which may be very important, are fugitive emissions from the nearby quarries. These quarries supply the cement plants with the raw materials necessary for cement production, and Ca is a marker for cement dust (Kim et al. 2004). Therefore, this source not only has a natural component but an anthropogenic one as well. The composition of the aforementioned enumerated sources is very similar, making it very difficult for PMF to separate them. Further spatial–temporal information would be necessary in order to be able to make such a separation. However, some information can be obtained by CPF calculations. Actually, as shown in Fig. 7, the areas that contribute most to the elevated values of this source are those located in a northwesterly direction where the cement plants and many of the quarries are situated, thus evidencing the importance of this contribution. Moreover, the Al/Ca ratio is much lower than in other nearby zones (Nicolás et al. 2008).

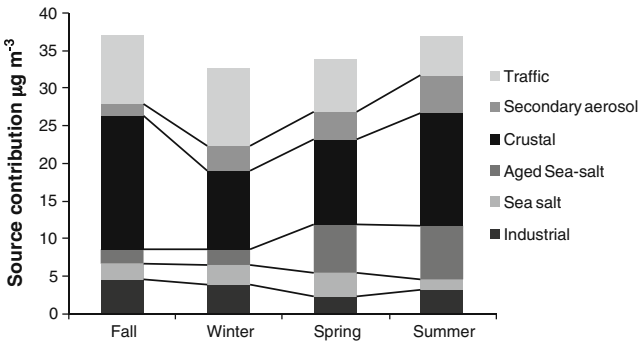

Fig. 6 Seasonal averages of the source contributions obtained by PMF

This is confirmed by the time trend of this source which shows four episodes with very high absolute concentrations of up to more than 50 μg/m^3 (on 5 September 2005, 9 November 2005, 10 March 2006, and 15 June 2006, indicated by arrows in Fig. 5). These days are characterized by strong NW winds caused by Atlantic fronts (a common occurrence in spring and fall) that may produce dust resuspension and transport from the cement plants and from the quarries.

As far as the average seasonal concentrations are concerned (Fig. 6), they have maximum values in summer and fall for several different reasons. In fall, this is due to the aforementioned episodes and to the numerous thermal inversions that favor contaminant accumulation. In summer, this is due to the great number of days under the influence of Saharan intrusions and to the scarce precipitation.

Traffic is the second most important source, characterized by NO_3^-, EC, OC, Cu, Pb, Sb, and Ba. The first three are mainly related with gases emitted via motor vehicle exhaust pipes and their posterior transformation into particles. Cu and Sb are related with tire and brake shoe abrasion. Pakkanen et al. (2001) identified Ba as one of the species markers of "road dust." Brake pads are commonly filled with $BaSO_4$, and antimony trisulfide (Sb_2S_3) is often added as a lubricant (Thorpe and Harrison 2008). Important quantities of crustal elements (like Ca and Fe) also appear in the source profile, whose explanation could be resuspended dust that had been previously deposited upon the pavement (Kim and Henry 2000). The traffic source constitutes about 20% of PM_{10} during the entire period,

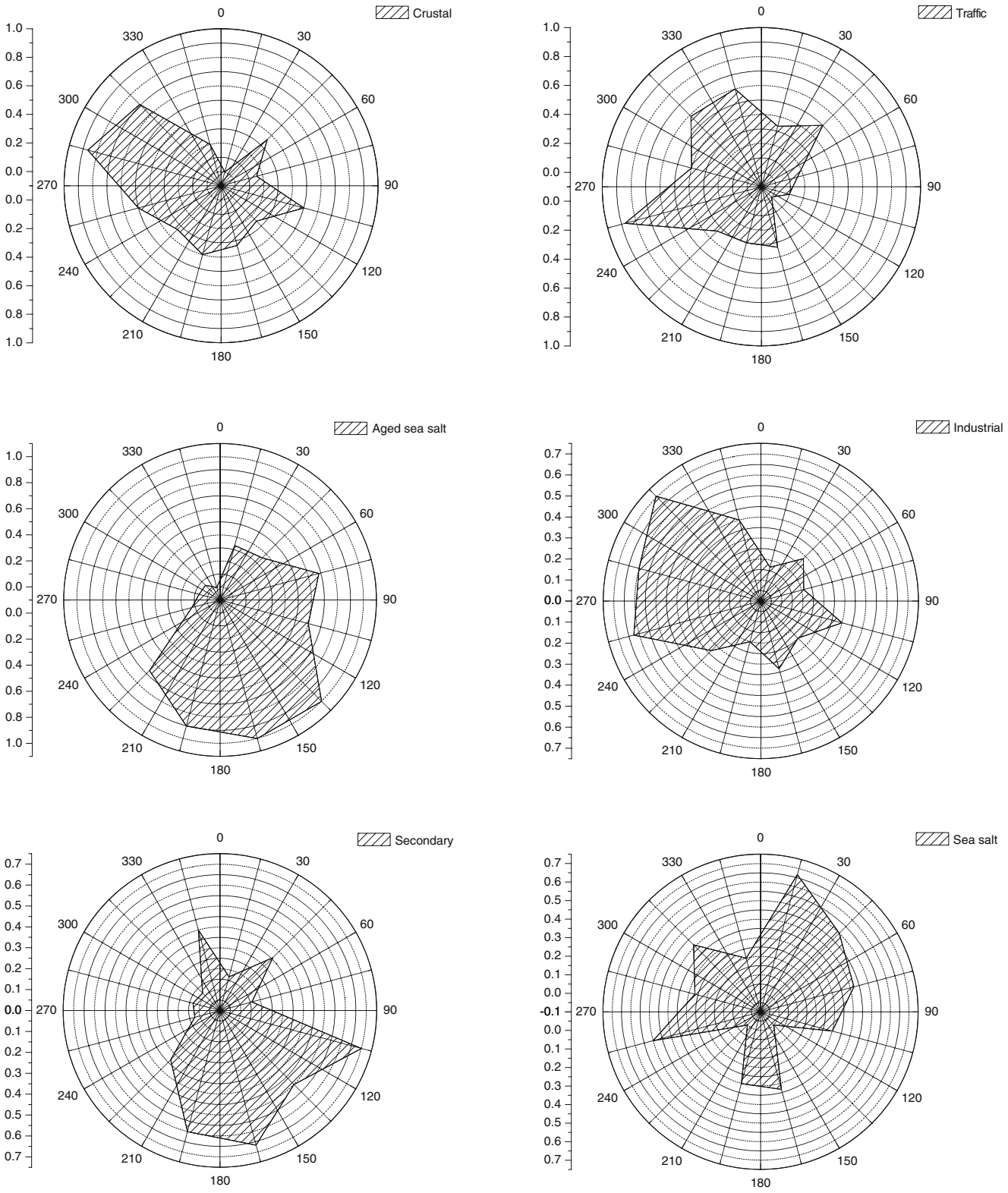

Fig. 7 CPF plots of the source contributions calculated by PMF

with an average of 7.9 μg m^{-3}. Its contribution is greater during fall and winter due primarily to a reduction in the mixing layer altitude during this period. In Fig. 5, the days 20 October 2005, 12 December 2005, 12 December 2006, 9 February 2006, and 31 March 2006 (indicated by arrows) are the main episodes of traffic origin and clear examples of days with very stable meteorological conditions. Because the sampling point is surrounded by primary roadways, the CPF plot indicates different directions, with the southwest, an area with the junction of two freeways, being the most important one.

Source 3 is primarily characterized by Na and soluble Mg. In fact, almost 70% of the measured Na has its origin in this source. The Na/Mg ratio of 8.7, which is similar to the ratio obtained for seawater (i.e., 8.3), indicates that these two elements originate from the same source and have a marine origin. The lack of Cl in this source indicates that some type of reaction is occurring to make it disappear: For this reason, we called this source "aged sea salt." Two reactions that might be responsible for the Cl disappearance are:

$HNO_3+NaCl \Rightarrow NaNO_3 + HCl$ (g)

$H_2SO_4+2NaCl \Rightarrow Na_2SO_4 +2HCl$ (g)

In both cases, particles rich in Na are obtained as a result. If the source profile is observed, important quantities of NO_3^- and SO_4^{2-} appear, indicating that these reactions are occurring. Furthermore, the first reaction is favored because ammonium nitrate breaks down at high temperatures, forming large quantities of nitric acid during summer. Figures 5 and 6 show that the contribution from this source is more important in spring and summer. In these seasons, local sea breeze circulations from the E–SE are the dominant meteorological conditions in the area. The CPF plot confirms that this source comes from the Mediterranean Sea in the SE direction; that is where the aforementioned transformations can occur while traversing the two cities surrounding the industrial zones. Aged sea salt contributes 11% to PM_{10} during the entire period, with an average of 4.4 μg m^{-3}.

The fourth source is characterized by elements like V or Ni, tracers from petroleum coke combustion (Pacyna 1986): So, it is due to industrial emissions. This source is highly linked to cement plants because the energy for kiln operations is produced from this type of combustion. The contribution is greater in winter than in summer because meteorological conditions make the dispersion of the industrial emissions more difficult. Industrial emissions contribute 9% to the PM_{10} value, and their average throughout the entire period was 3.5 μg m^{-3}. The directions where the two cement plants are located have a high CPF value (Fig. 7).

Large quantities of NH_4^+ and SO_4^{-2} characterize the fifth source and clearly represent the presence of ammonium sulfate in the area (Nicolás et al. 2009b; Galindo et al. 2008) from photooxidation of sulfuric oxides initially emitted as gases from local emissions (for example the cement plant) and long-distant transport. The NH_4^+ presence is not large enough to neutralize the entire existing sulfate in the atmosphere. Its seasonal evolution is typical, with high values in summer when photochemical activity is greater. This source explains 8% of PM_{10} with an annual average of 3.4 μg m^{-3}.

Finally, marine aerosol represents the last source, characterized by large quantities of Cl, Na, and soluble Mg. It accounts for 6% of PM_{10} with an annual average of 2.3 μg m^{-3}. This source primarily represents the quantity of unreacted NaCl. Therefore, its concentration is lower in summer due to the chemical reactions favored during this season. The CPF plot shows wind directions that also come from the sea, albeit different from those obtained for the aged sea salt source. The highest episodes from that source, 11 April 2006, 09 May 2006, and 1 June 2006 (see arrows in Fig. 5), correspond to specific synoptic meteorological conditions of NE winds from the Mediterranean Sea.

4 Summary

The contributions to PM_{10} from different types of sources were quantified in a residential area located near an industrial zone primarily constituted by cements plants, in southeastern Spain, by PMF applied to a data set that includes elements, ions, and carbonaceous species.

The interpretation of PMF results has been improved by the study of the CPFs, i.e., by connecting the source contributions with meteorological factors (wind direction and velocity): In particular, it allowed us to understand which sources are connected to the industrial emissions coming from the NW direction.

The main contribution to PM_{10} (34%) is due to the crustal source, which may have different origins: Saharan intrusions, fugitive emissions escaping the cement plant installations or quarries, local dust resuspended by the wind, or traffic. However, the combined use of PMF and CPF highlighted a predominant contribution from the industrial pole.

Consequently, the cement plants' contribution to PM_{10} concentration levels is not solely represented by the cement plant combustion of petroleum coke, but in great measure by a crustal component as well. Therefore, in order to reduce PM_{10} levels, the application of reduction techniques to lessen fugitive emissions would be additionally necessary.

The traffic source, which provides an average contribution of 20%, is a result of both vehicle exhaust and emissions from tire and break wear. Secondary sulfates accounts for 8% of PM_{10} concentration.

Finally, two sea salt sources have been identified (with a global average contribution of 7%): a fresh marine aerosol and an aged one, characterized by Cl depletion (and SO_4 and NO_3 enrichment) due to chemical reactions taking place in the atmosphere.

Concerning seasonability, sources such as aged sea salt and secondary aerosol present elevated values in summer, while others like traffic and industrial were highest during winter. For the former, this is due to photochemical reactions being favored during this time of year that form this type of aerosol; for the latter group, meteorological situations occur in fall and winter, which allow the accumulation of contaminants.

Acknowledgments We thank the Elche City Hall for allowing access to their facilities for the placement of the instruments, the Air Quality Surveillance Network of the Valencian Community Regional Government for supplying data, and Paul Nordstrom and Guillermo Escribano for their assistance in this work. This work was funded by research project from the Spanish Ministry of Environment (GRACCIE-CSD2007-00067)

References

Abbey DE, Nishino N, McDonell WF, Burchette RJ, Knutsen SF, Beeson WL et al (1999) Long-term inhalable particles and other air pollutants related to mortality in nonsmokers. Am J Respir Crit Care Med 159:373–382

Amato F, Pandolfi M, Escrig A, Querol X, Alastuey A, Pey J et al (2009) Quantifying road dust resuspension in urban environment by Multilinear Engine: a comparison with PMF2. Atmos Environ 43:2770–2780

Ashbaugh LL, Malm WC, Sadeh WZ (1985) A residence time probability analysis of sulfur concentrations at Grand Canyon national park. Atmos Environ 19:1263–1270

Begum AB, Kim E, Biswas SK, Hopke PK (2004) Investigation of sources of atmospheric aerosol at urban and semi-urban areas in Bangladesh. Atmos Environ 38:3025–3038

Birch ME, Cary RA (1996) Elemental carbon-based method for monitoring occupational exposures to particulate diesel exhaust. Aerosol Sci Tech 25:221–241

Dockery DW, Pope CA III (1994) Acute respiratory effects of particulate air pollution. Annu Rev Publ Health 15:107–132

Galindo N, Nicolás JF, Yubero E, Caballero S, Pastor C, Crespo J (2008) Factors affecting levels of aerosol sulfate and nitrate on the Western Mediterranean coast. Atmos Res 88:305–313

Hopke PK, Lamb RE, Natusch D (1980) Multielemental characterization of urban roadway dust. Environ Sci Technol 14:164–172

Huerbert BJ, Charlson RJ (2000) Uncertainties in data on organics aerosols. Tellus B 52:1249–1255

Kim BM, Henry RC (2000) Application of SAFER model to the Los Angeles PM_{10} data. Atmos Environ 34:1747–1759

Kim KH, Hopke PK (2004a) Comparison between conditional probability function and nonparametric regression for fine particle source directions. Atmos Environ 38:4667–4673

Kim E, Hopke PK (2004b) Source apportionment of fine particles at Washington, DC utilizing temperature resolved carbon fractions. J Air Waste Manage 54:773–785

Kim E, Hopke PK, Edgerton ES (2004) Improving source identification of Atlanta aerosol using temperature resolve carbon fractions in positive matrix factorization. Atmos Environ 38:3349–3362

Lippmann M (1998) The 1997 US EPA standards for particulate matter and ozone. In: Hester RE, Harrison RM (eds) Issues in environmental science and technology, 10. Royal Society of Chemistry, London, pp 75–99

Natusch DFS, Wallace JR, Evans CA Jr (1974) Toxic trace elements: preferential concentration in respirable particles. Science 183:202–204

Nicolás J, Chiari M, Crespo J, Garcia Orellana I, Lucarelli F, Nava S et al (2008) Quantification of Saharan and local dust impact in an arid Mediterranean area by the positive matrix factorization (PMF) technique. Atmos Environ 42:8872–8882

Nicolás J, Yubero E, Galindo N, Gimenez J, Castañer R, Carratalá A et al (2009a) Characterization of events by aerosol mass size distributions. J Environ Monit 11:394–399

Nicolás J, Galindo N, Yubero E, Pastor C, Esclapez R, Crespo J (2009b) Aerosol inorganic ions in a Semiarid region on the southeastern Spanish Mediterranean coast. Water Air Soil Poll 201:149–159

Pacyna JM (1986) Emission factors of atmospheric elements. In: Nriagu JO, Davidson CI (eds) Toxic metals in the atmosphere. Wiley, New York, pp 33–52

Paatero P (1997) Least squares formulation of robust non-negative factor analysis. Chemometr Intell Lab 38:223–242

Paatero P (2004) User's guide for positive matrix factorization programs PMF2 and PMF3, Par. 1: tutorial

Paatero P, Tapper U (1994) Positive matrix factorization: a non-negative factor model with optimal utilization of error estimates of data values. Environmetrics 5:111–126

Paatero P, Hopke PK (2003) Discarding or downweighting high-noise variables in factor analytic models. Anal Chim Acta 490:277–289

Paatero P, Hopke PK, Song X, Ramadan Z (2002) Understanding and controlling rotations in factor analytic models. Chemometr Intell Lab 60:253–264

Pakkanen T, Loukkola K, Korhonen C, Aurela M, Mäkelä T, Hillamo R et al (2001) Sources and chemical composition of atmospheric fine and coarse particles in the Helsinki area. Atmos Environ 35:5381–5391

Polissar AV, Hopke PK, Paatero P, Malm WC, Sisler JF (1998) Atmospheric aerosol over Alaska 2. Elemental composition and sources. J Geophys Res 103(D15):19045–19057

Qin Y, Oduyemi K, Chan LY (2002) Comparative testing of PMF and CFA models. Chemometr Intell Lab 61:75–87

Querol X, Alastuey A, Moreno T, Viana MM, Castillo S, Pey J et al (2008) Spatial and temporal variations in airborne particulate matter (PM_{10} and $PM_{2.5}$) across Spain 1999–2005. Atmos Environ 42:3964–3979

Salvador P, Artiñano B, Querol X, Alastuey A, Costoya M (2007) Characterisation of local and external contributions of atmospheric particulate matter at a background coastal site. Atmos Environ 41:1–17

Tauler R, Viana M, Querol X, Alastuey A, Flight RM, Wentzell PD et al (2009) Comparison of the results obtained by four receptor modeling methods in aerosol source apportionment studies. Atmos Environ 43:3989–3997

Thorpe A, Harrison RM (2008) Sources and properties of non-exhaust particulate matter from road traffic: a review. Sci Total Environ 400:270–282

Viana M, Kuhlbusch TAJ, Querol X, Alastuey A, Harrison RM, Hopke PK et al (2008) Source apportionment of particulate matter in Europe: a review of methods and results. J Aerosol Sci 39:827–849